

# Advancing Particle Identification in Helium-Based Drift Chambers: A Cluster Counting Technique Study through Beam Tests

**W. Elmetenawee,<sup>a,\*</sup> M. Abbrescia,<sup>a,b</sup> M. Anwar,<sup>a,d</sup> A. Corvaglia,<sup>c</sup> B. D'Anzi,<sup>a,b</sup> N. De Filippis,<sup>a,d</sup> F. De Santis,<sup>c</sup> E. Gorini,<sup>c,e</sup> F. Grancagnolo,<sup>c</sup> F. Gravili,<sup>c,e</sup> M. Louka,<sup>a,b</sup> A. Miccoli,<sup>c</sup> M. Panareo,<sup>c,e</sup> M. Primavera,<sup>c</sup> Francesco Procacci<sup>a</sup> and A. Ventura<sup>c,e</sup>**

<sup>a</sup>*Istituto Nazionale di Fisica Nucleare Sezione di Bari, Via E. Orabona 4, 70126 Bari, Italy*

<sup>b</sup>*Dipartimento di Fisica - Universit'a di Bari Aldo Moro, Via E. Orabona 4, 70126 Bari, Italy*

<sup>c</sup>*Istituto Nazionale di Fisica Nucleare Sezione di Lecce, Via Arnesano, 73100 Lecce, Italy*

<sup>d</sup>*Politecnico di Bari, Via Amendola 126/b, 70126 Bari, Italy*

<sup>e</sup>*Dipartimento di Matematica e Fisica "Ennio De Giorgi" - Universit'a del Salento, Via Arnesano, 73100 Lecce, Italy*

*E-mail:* [walaa.elmetenawee@ba.infn.it](mailto:walaa.elmetenawee@ba.infn.it)

While the ionization process by charged particles ( $dE/dx$ ) is commonly used for particle identification, uncertainties in total energy deposition limit particle separation capabilities. To overcome this limitation, the cluster counting technique ( $dN/dx$ ) leverages the Poisson nature of primary ionization, providing a statistically robust method for inferring mass information. Simulation studies using Garfield++ and Geant4 indicate that the cluster counting technique can achieve twice the resolution of the traditional  $dE/dx$  method in helium-based drift chambers. However, in real experimental data, finding electron peaks and identifying ionization clusters is extremely challenging due to the superimposition of signals in the time domain. To address these challenges, this paper introduces cutting-edge algorithms and modern computing tools for electron peak identification and ionization cluster recognition in experimental data. The effectiveness of the algorithms is validated through four beam tests conducted at CERN, involving different helium gas mixtures, varying gas gains, and various wire orientations relative to ionizing tracks. The tests employ a muon beam ranging from 1 GeV/c to 180 GeV/c, with drift tubes of different sizes and diameter sense wires. The data analysis results concerning the ascertainment of the Poisson nature of the cluster counting technique, the establishment of the most efficient cluster counting and electrons clustering algorithms among the various ones proposed, and the dependence of the counting efficiency versus the beam particle impact parameter will be discussed. Additionally, a study comparing the resolution obtained using the  $dN/dx$  and  $dE/dx$  methods will be presented.

*42nd International Conference on High Energy Physics (ICHEP2024)*

*18-24 July 2024*

*Prague, Czech Republic*

---

\*Speaker

## 1. The cluster counting technique

In Helium-base gas mixtures, the ionization electrons generated by a charged track in a gas detector and collected at the anode are generally separated in time from a few nanoseconds to a few tens of nanoseconds, according to the electron collection geometry and to the electric field intensity. An efficient identification of these electrons can be accomplished using fast read-out electronics. As a consequence, by counting the total number of ionization events along a charged track ( $dN/dx$ ) [1], particle types can be identified with superior resolution compared to conventional methods based on the integral of the total energy losses ( $dE/dx$ ).

Analytical evaluations, reported in Figure 1 (left), demonstrate that the cluster counting technique enhances particle separation capabilities by a factor of 2 compared to the  $dE/dx$  technique. The plot illustrates particle separation power in terms of standard deviations ( $\sigma$ ) as a function of momentum in a gas mixture of 90% He and 10%  $iC_4H_{10}$ . The calculations assume an efficiency 80% for cluster counting. The technique exhibits excellent performance across the entire momentum range, experiencing only minor gaps in specific momentum intervals. The combination of the cluster counting and time-of-flight techniques as obtained from the DELPHES fast simulation is displayed in Figure 1 (right) and shows an efficient separation of  $K/\pi$  ( $\geq 3\sigma$ ) for momenta  $p < 30$  GeV.

A dedicated simulation analysis is developed to investigate the capabilities of the cluster counting technique and the ionization processes in a helium-based drift chamber [2, 3], utilizing both Garfield++ and Geant4 [4]. The simulation outcomes confirm that the cluster counting method enhances particle separation compared to the conventional  $dE/dx$  approach. Nonetheless, slight variations are observed between the separation powers predicted by Geant4 and Garfield++. Additionally, there is a notable absence of experimental data on cluster density and population for helium-based gases. Therefore, experimental validation is crucial to confirm the effectiveness of the cluster counting technique and to verify the simulation results.

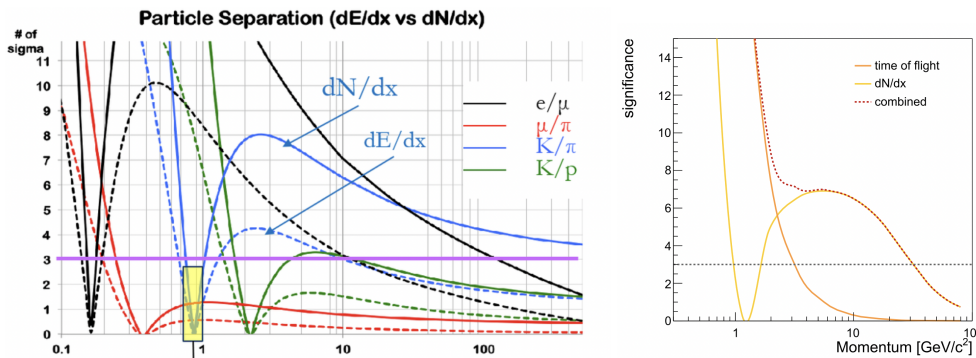


**Figure 1:** Left: Analytic evaluation of particle separation capabilities achievable with  $dE/dx$  (solid curves) and  $dN/dx$  (dashed curves). The region between 0.85 GeV/c and 1.05 GeV/c where a different technique is needed is highlighted in yellow. Right:  $K/\pi$  separation in number of  $\sigma$  as a function of the particle momentum using the  $dN/dx$  and time-of-flight methods.

## 2. Beam test setup

Several sets of square cross-section brass drift tubes, ranging in size from 1.0 to 3.0 cm, are equipped with sense wires of varying diameters from 10 to 40  $\mu\text{m}$ . These tubes are operated at gas gains between 1 and  $5 \times 10^5$ , filled with Helium-Isobutane gas mixtures in ratios of 90/10, 85/15, and 80/20, and exposed to muon beams with different momenta during four beam test campaigns.

In November 2021 and July 2022, the beam test occurred at CERN in the SPS-H8 beamline with muons on the Fermi plateau from 40 to 180 GeV/c. In July 2023 and July 2024, the beam test occurred at CERN in the PS-T10 beamline with muons on the relativistic rise, ranging from 2 to 10 GeV/c. Figure 2 (left) provides an overview of these beam test campaigns at CERN, alongside earlier pioneering measurements from a beam test at PSI conducted several years ago.

Figure 2 (right) shows an upstream view of the beamline, depicting the 2021 beam test setup, where the drift tubes (shielded by copper tape) are installed along with the rest of the experimental apparatus. Similar configurations are employed for the subsequent beam tests.

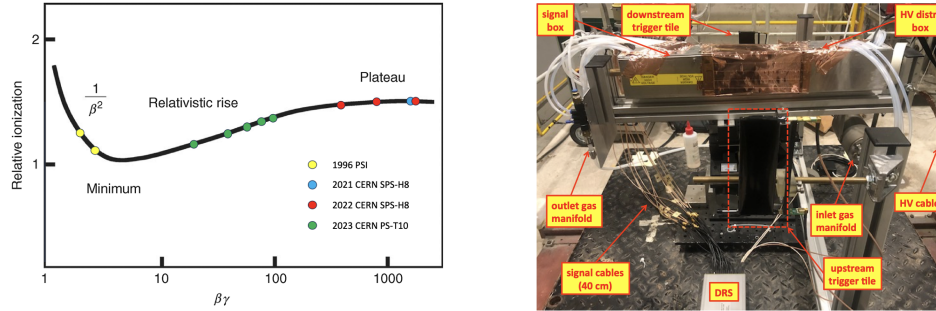


**Figure 2:** Left: Beam test campaigns with muons of the indicated  $\beta\gamma$  values over imposed to a generic Bethe-Block curve. Right: The experimental setup seen from the beam upstream. The main components of the setup are indicated by the yellow insets

## 3. Results

Defining the operating parameters of the various drift tubes under different conditions—particularly the gas gain, which determines the single electron pulse height—is a crucial preliminary step for ensuring homogeneous data collection when evaluating the efficiency of different cluster counting algorithms.

### 3.1 Gas gain

The gas gain as a function of the anode high voltage (HV) has been determined by fitting the single electron pulse height with a Landau distribution. The fitted most probable value (MPV) was then corrected for the amplifier gain, the impedance mismatch between the characteristic tube impedance and the 330  $\Omega$  termination resistor, and the current divider effect between the 330  $\Omega$  termination resistor and the 50  $\Omega$  input impedance of the ADC.

Figure 3 shows the gas gain plotted as a function of the anode HV for the different configurations used for 1 cm drift tubes in the 2022 beam test at 725 Torr absolute pressure. The data indicate that,

for effective application of cluster counting techniques, the optimal range of gas gain—regardless of drift tube configuration (drift length, sense wire diameter, gas mixture)—lies between  $1 \times 10^5$  and  $5 \times 10^5$ .

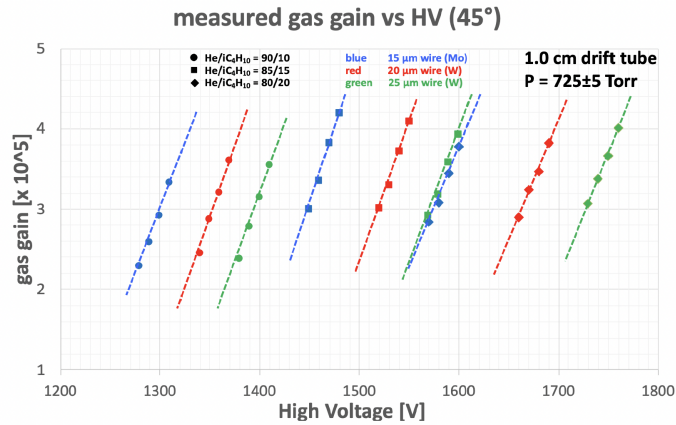


**Figure 3:** Gas gain as a function of the anode high voltage based on July 2022 test beam data for 1 cm drift tubes. The  $45^\circ$  angle refers to the angle between the beam direction and the normal to the sense wire. Different gas mixtures are represented by distinct symbols, while various sense wire diameters are indicated by different colors.

### 3.2 Electron Peak Finding

The results presented in this paper are obtained using two distinct methods for electron peak-finding. Before applying these methods, a preprocessing step is performed on the beam test data to set the waveform baseline to zero. This is done by subtracting to the waveform the mean value of the pulse height averaged over the first 30 ns, a time interval outside of the signal acceptance. Its root mean square (r.m.s.), of over the same time interval, defines the noise value.

The first peak-finding technique employed is a derivative-based algorithm (DERIV). This method calculates the first derivative as the difference of the waveform amplitude between two consecutive bins and the second derivative as the difference of the first derivative between the same bins. To identify a peak candidate, the algorithm requires that the first derivative at the peak candidate position is less than a pre-defined quantity, proportional to a value propagated by the r.m.s. noise, and that increases before and decreases after the peak candidate position within a margin proportional to the r.m.s. noise. As a further requirement, the waveform concavity is checked with the second derivative. Additionally, the algorithm imposes amplitude thresholds, based on the r.m.s., for the peak candidate and thresholds on the amplitude difference between the peak candidate and its neighbouring bins.

The second peak-finding method is the Running Template Algorithm (RTA). This approach defines an electron pulse template, characterized by rising and falling exponentials, over a fixed number of bins derived from experimental data and digitized according to the sampling rate. The RTA scans the data waveform, comparing the normalized electron pulse template to the data within a search window. It evaluates the agreement between the template and the data, applying a cut-off to identify peaks. Once a peak is found, it is subtracted from the signal, and the process repeats until no further peaks are detected.

Figure 4 presents an illustration of the peaks identified by the two aforementioned algorithms. A third very promising approach at identifying ionization clusters in the signal waveform is obtained with the application of ML techniques [5].

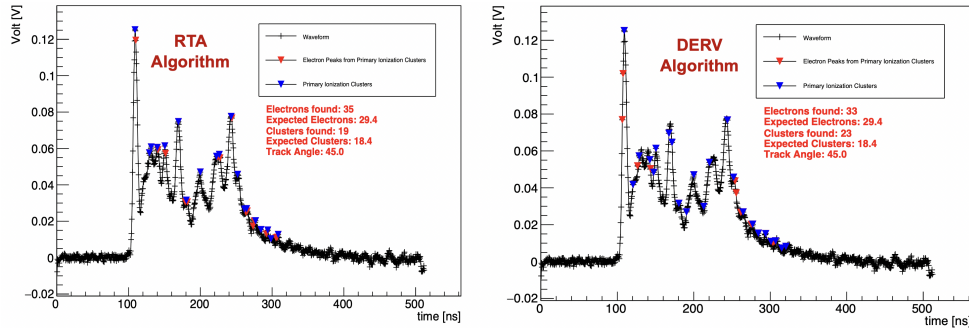


**Figure 4:** Data waveform recorded for a 1 cm drift cell with a  $20\ \mu\text{m}$  sense wire diameter, a  $45^\circ$  track angle, a sampling rate of 2 GSa/s, and a He/iC<sub>4</sub>H<sub>10</sub> 90/10 gas mixture. The RTA algorithm (left) and DERV algorithm (right) are used for electron peak identification, with cluster peaks indicated by blue arrows and electron peaks by red arrows.

### 3.3 Clusterization

The process of identifying primary ionization clusters, referred to as "clusterization," involves grouping together all ionization electrons generated in the same ionization act. This process associates peaks identified in the signal waveform by the described algorithms into clusters, defining a drift time and amplitude for each.

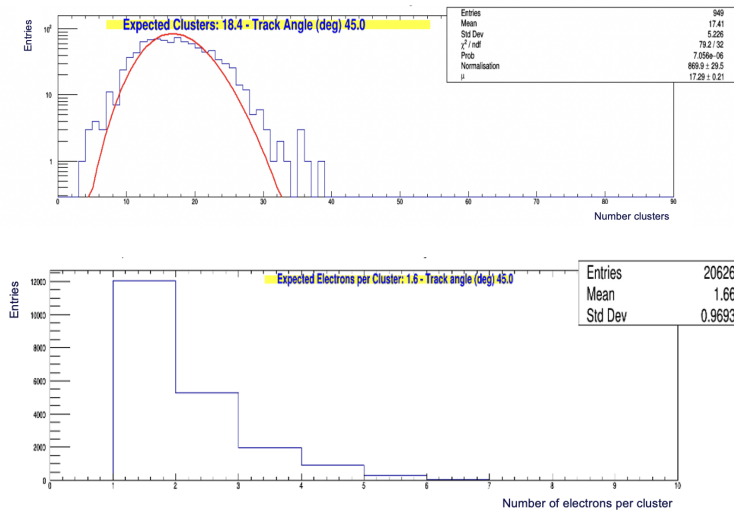
The procedure is as follows: contiguous electron peaks, with relative time differences compatible with the time spread due to diffusion, are grouped into the same ionization cluster. The electron count for each cluster is incremented accordingly. The cluster's drift time and amplitude are arbitrarily set to those of the electron with the highest amplitude within the cluster. An illustration of the peaks identified by the two algorithms in a single waveform is shown with blue markers in Figure 4.

Figure 5 (left) displays the cluster distribution determined by the clustering algorithm. The red line superimposed on the plots represents the result of a fit to a Poisson function, with the mean value consistent with expectations.

Consistency checks on the reliability of the applied procedures are carried out by examining the electron cluster population. Figure 5 (right) shows the average number of electrons per cluster, which aligns well with the experimental measurements [6].

### 3.4 Performance scans

Using test beam data, we evaluated the performance of our algorithms across a range of operational conditions, including gas mixtures, gain, geometrical configurations (such as cell size and sense wire dimensions), sampling rate, high voltage (HV), and track angle. This section presents scans of cluster counting efficiency, providing key insights into how various parameters—gas gain, angle, and gas composition—impact the drift chamber's ability to detect ionization clusters.



**Figure 5:** Distribution of the number of clusters (top) and the number of electrons per cluster (bottom) for a 1 cm drift cell with a 20  $\mu\text{m}$  sense wire diameter, a 45° track angle, a sampling rate of 2 GSa/s, and a He/iC<sub>4</sub>H<sub>10</sub> 90/10 gas mixture by applying the RTA + clusterization algorithm.

To account for differences in drift velocities across different gas mixtures, the clusterization cuts are optimized individually for each mixture. Figure 6 (left) displays the efficiency of the cluster counting for the three different helium-isobutane gas mixtures: 90/10, 85/15, and 80/20. The results are consistent with the expected specific ionizations, producing approximately 12, 15, and 18 clusters per cm per minimum ionizing particle (m.i.p.), respectively.

Additionally, we examined how the number of clusters scales with track length by comparing results at varying beam angles. Figure 6 (middle) presents the ratio of counted clusters to expected clusters as a function of beam angle for two gas mixtures. The observed cluster deficit at normal incidence for the 80/20 gas mixture is likely due to space charge effects, while at large angles, the higher ionization electron densities affect the efficiency of the cluster counting algorithms.

Figure 6 (right) shows the relationship between counting efficiency and gas gain, with each step in the HV configuration corresponding to approximately a 20% variation in gain. A slight dependence of counting efficiency on gas gain is observed, highlighting the sensitivity of the detection process to gain variations. It is worth to mention that all peak finding parameters used for this analysis are optimized for the HV configuration 0 and undercounting and overcounting can be corrected by slight modifications of these parameters.

### 3.5 Resolution study

This section presents a comparative analysis of the resolution obtained from the measurement of charge deposits along a particle's track ( $dE/dx$ ) and the ionization clusters ( $dN/dx$ ), using identical tracks made of the same hits for both methods.

The measurement of energy loss along a particle's track,  $dE/dx$ , follows a Landau distribution, characterized by a long tail caused by high-energy  $\delta$  electrons. To calculate the energy loss, the charge deposited in multiple drift cells along the track is recorded, and the mean charge of these samples is taken as the  $dE/dx$  value. However, this simple mean is sensitive to large fluctuations



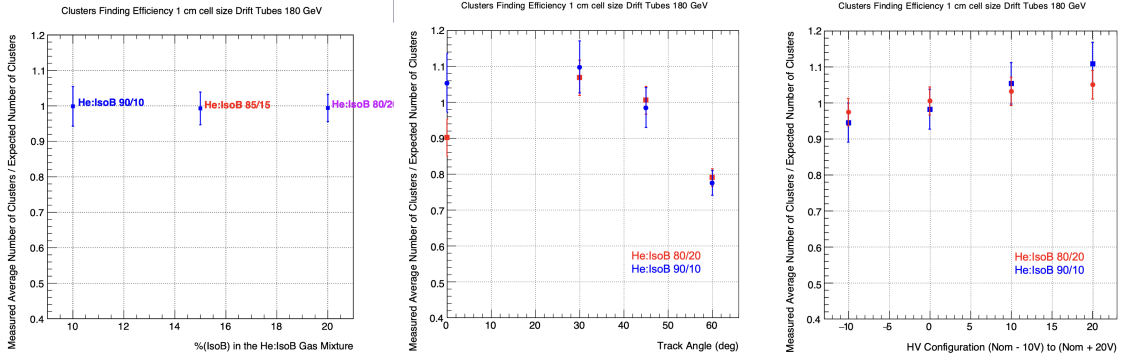


**Figure 6:** Comparison plots showing the cluster counting efficiency as a function of gas mixture (left), track angle (middle), and drift tube high voltage settings (right) using the RTA + clusterization algorithm.

due to the nature of the Landau distribution, where outliers with high charge deposits can skew the result. To address this, the truncated mean method is employed, discarding the highest charge samples—typically the top 20-30%—and calculating the mean of the remaining samples. The truncation threshold is empirically optimized to achieve the best  $dE/dx$  resolution, with the optimal configuration retaining 80% of the charge distribution.

The resolution of  $dN/dx$  is estimated using the same tracks employed for the  $dE/dx$  analysis. The RTA + clusterization algorithm, as described in Section 2, is applied to reconstruct the ionization clusters. The truncated charge distribution was then compared with the number of ionization clusters measured along a 2-meter track length, as shown in Figure 7. The results demonstrate that the  $dN/dx$  method achieves a resolution of 3%, which is nearly twice as good as the 5.7% resolution obtained from the  $dE/dx$  method, in agreement with both analytical calculations and simulation predictions.

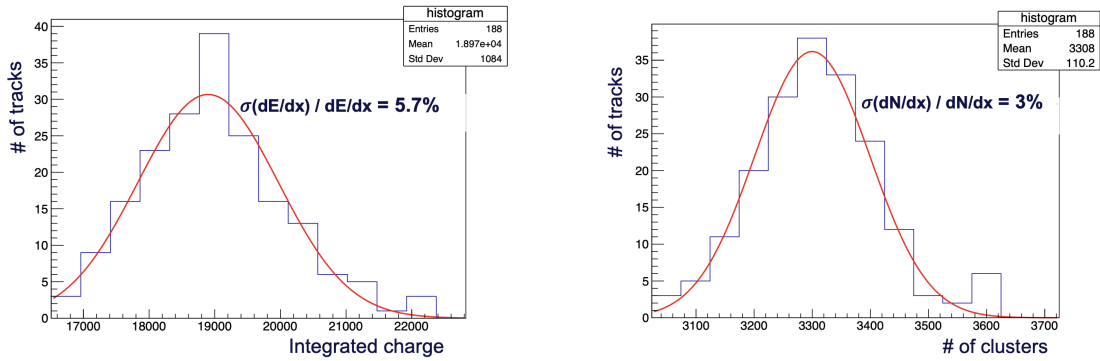


**Figure 7:** The integral of the truncated mean charge distribution at 80% (left) and the number of ionization clusters (right) measured along 2-meter tracks made of the same hits. The red lines superimposed on the plots represent the result of Gaussian fit.

Furthermore, the resolution is evaluated for different track lengths, as shown in Figure 8, for both the  $dE/dx$  and  $dN/dx$  methods. The resolution dependence on track length is found to follow the  $L^{-0.37}$  scaling for  $dE/dx$ , consistent with the Lehraus plot [7], and the  $L^{-0.5}$  scaling for  $dN/dx$ , highlighting the superior resolution offered by the cluster counting technique.

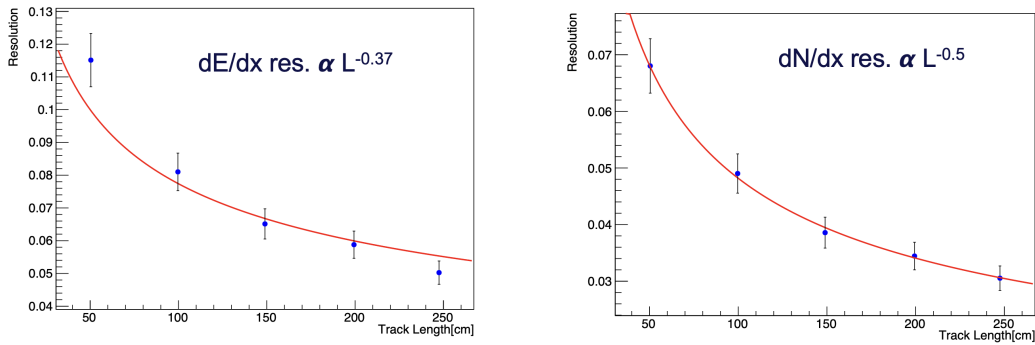


**Figure 8:** Resolution as a function of track length (L) for the dE/dx method (left) and dN/dx method (right). The red lines superimposed on the plots show the fits of  $L^{-0.37}$  for dE/dx and  $L^{-0.5}$  for dN/dx.

#### 4. Conclusions

The cluster counting technique has demonstrated significant potential for improving particle identification capabilities, as confirmed by both analytical evaluations and simulations. Two key algorithms, DERV and RTA, are developed to detect electron peaks and delivered results closely aligned with expectations. The performance of these algorithms is evaluated using test beam data under various conditions. A resolution study confirmed that the dN/dx method achieved resolution twice as good as that of the traditional dE/dx method, consistent with theoretical predictions. Further insights, particularly in the relativistic rise region, are anticipated from the upcoming 2024 test beam results.

#### References

- [1] G. Cataldi et al., Cluster counting in helium based gas mixtures, Nuclear Instruments and Methods in Physics Research A 386 (1997) 458-469.
- [2] G.F. Tassielli on behalf of the IDEA Collaboration, A proposal of a drift chamber for the IDEA experiment for a future e+e- collider Volume ICHEP2020, PoS. (2021) 877.
- [3] W. Elmetenawee et al., The Tracking performance for the IDEA drift chamber. PoS ICHEP2022, 362 (2022). <https://doi.org/10.22323/1.414.0362>
- [4] F. Cuna et al., Simulation of particle identification with the cluster counting technique. ArXiv. /abs/2105.07064 (2021).
- [5] G. Zhao et al., Peak finding algorithm for cluster counting with Domain Adaptation, to be published on Computer Physics Communications, COMPHY-D-24-00084.
- [6] H. Fischle, J. Heintze and B. Schmidt, Experimental Determination of ionisation Cluster Size Distribution in counting Gases, Nucl. Instr. Meth. A 301 (1991).
- [7] I. Lehraus et al., Particle identification by dE/dx sampling in high pressure drift detectors, Nucl. Instr. Meth., 196 (1982) 361.